



Grading of Glioma Tumors by Analysis of Minimum Apparent Diffusion Coefficient and Maximum Relative Cerebral Blood Volume

Saberi Mahdiyeh (MSc)¹, Faeghi Fariborz (PhD)^{2*}, Ghanaati Hossein (MD)³, Miri Mojtaba (MD)⁴, Rostamzadeh Ayoob (MSc)⁵, Khodakarim Soheila (PhD)⁶, Naleini Farhad (MD)⁷

ARTICLE INFO

Article type:
Original Article

Article history:
Received: 5 November 2015
Accepted: 8 February 2016
Available online: 6 March 2016
CJNS 2016; 2 (4): 42-53

1. Medical Imaging Physicist, Department of Radiology Technology, Faculty of Allied Medical Sciences, Shahid Beheshti University of Medical Sciences, Tehran, Iran
2. Medical Physicist, Assistant Professor of Medical Imaging, Department of Radiology Technology, Faculty of Allied Medical Sciences, Shahid Beheshti University of Medical Sciences, Tehran, Iran
3. Radiologist, Advanced diagnostic and Interventional Radiology Research Center (ADIR), Tehran University of Medical Sciences, Tehran, Iran
4. Neurosurgen, Department of Neurosurgery, Emam Khomeini Hospital, Tehran University of Medical Sciences, Tehran, Iran
5. Neuroscientist, Funding Member of Iranian Society of Cellular and Molecular Imaging, Department of Anatomy and Neuroscience, Faculty of Medicine, Shahrekord University of Medical Sciences, Shahrekord, Iran
6. Epidemiologist, Department of Epidemiology, Shahid Beheshti University of Medical Sciences, Tehran, Iran
7. Radiologist, Emam Reza Hospital, Faculty of Medicine, Krmanshah University of Medical Sciences, Krmanshah, Iran

***Corresponding author:**
Medical Physicist, Assistant Professor of Medical Imaging, Department of Radiology Technology, Faculty of Allied Medical Sciences, Shahid Beheshti University of Medical Sciences, Tehran, Iran
Email: f_faeghi@sbmu.ac.ir

ABSTRACT

Background: Gliomas are the most common primary neoplasms of the central nervous system. Relative cerebral blood volume (rCBV) could estimate high-grade Gliomas computed with dynamic susceptibility contrast MR imaging which it is artificially lowered by contrast extravasation through a disrupted blood-brain barrier.

Objectives: Our intent was to clarify the usefulness of diffusion-weighted magnetic resonance imaging (DWI) and perfusion weighted magnetic resonance imaging (PWI) in the grading of Gliomas.

Materials and Methods: Both PWI and DWI with a three-tesla scanner investigated nineteen consecutive patients with Gliomas. The means of rCBV and ADC values have been compared among the tumor groups with t-test and ROC curve analysis to determine threshold values of Gliomas grading.

Results: Mean maximum rCBV were 2.71 ± 1.41 for low grades (I & II), and 8.14 ± 2.58 for high grades (III & IV) Gliomas ($p=0.001$). Mean minimum ADC were $1.47 \pm .46 \times 10^3 \text{ mm}^2/\text{s}$ for low grades (I & II), and $.47 \pm .38 \times 10^3 \text{ mm}^2/\text{s}$ for high grades (III & IV) Gliomas ($p=0.001$). We can get $0.94 \times 10^3 \text{ mm}^2/\text{s}$ for minimum ADC and 3.85 for maximum rCBV as a difference cutoff point between low and high-grade Gliomas.

Conclusion: Combination of both DWI and PWI techniques, with measurement of minimum ADC and maximum rCBV can be used to distinguish between high grade and low-grade Glioma tumors.

Keywords: Diffusion Magnetic Resonance Imaging; Neoplasm Grading

Copyright © [2016] Caspian Journal of Neurological Sciences. All rights reserved.

➤ **Please cite this paper as:**

Saberi M, Faeghi F, Ghanaati H, Miri M, Rostamzadeh A, Khodakarim S, Naleini F. Grading of Glioma Tumors by Analysis of Minimum Apparent Diffusion Coefficient and Maximum Relative Cerebral Blood Volume. Caspian J Neurol Sci 2016; 2(4):42-53.

Introduction

Gliomas are the most common primary neoplasms of the central nervous system and are classified into four

grades by the World Health Organization (WHO) (1,2). Tumor grading has critical implications for preoperative planning

therapeutic approaches, subsequent follow-up care, and assessing the patient prognosis and response to therapy (3). However, conventional magnetic resonance imaging (MRI) alone is not always accurate in predicting Glioma grade. Glioma grading is based on the histopathological assessment (3). Advanced MR imaging techniques such as DSC (Dynamic Susceptibility Contrast) and Diffusion Weighted Imaging (DWI) provide physiologic information that complements the anatomic information obtained from conventional MRI (3,4). Diffusion is a term used to describe the movement of molecules due to random thermal motion restricted by boundaries such as ligaments, membranes and macromolecule. Sometimes restrictions in diffusion are directional, depending on the structure of the tissues. Diffusion of molecules also occurs across tissues, especially from areas of restricted diffusion to areas with free diffusion (3,5). The comprehensive displacement of molecules is called the apparent diffusion coefficient (ADC) and a sequence can be sensitized to this motion by applying two gradients on either side of the 180° radiofrequency (RF) pulse. This works in the similar way to phase contrast Magnetic Resonance Angiography (MRA) in that stationary spins will acquire no net phase change after applying the gradients. Moving spins, however, will acquire this phase change and result in a signal loss. In diffusion imaging, normal tissue has lower signal intensity than abnormal tissue, as the molecules within it are free to move, while diffusion becomes restricted when there is a pathologic change. The signal change depends on the ADC (Apparent Diffusion Coefficient) of the tissue and the strength of the gradients. Their amplitude are controlled by the b factor/value which is similar to the VENC (Encoding Velocity) in phase contrast MRA

(4,5). This is another type of weighting in diffusion imaging; an extrinsic contrast parameter (b factor) controls how much a tissue's ADC contributes towards image weighting. If the TE (echo time) and TR (repetition time) are long and b=zero image is T2 weighted. If we then increase the b factor, then the image weighting changes from T2 to diffusion weighting. By this, we mean that areas will have a high signal not because they have a long T2 time but because they have a low ADC. This is why this technique is called diffusion weighted imaging. It is, in fact, another type of weighting. 'b' is expressed in units of s/mm^2 (6). ADC maps are acquired via post-processing by calculating the ADC for each voxel of tissue and allocating signal intensity according to its value. Therefore, restricted tissue, which has a low ADC, is darker than free diffusing areas that have a high ADC (7). The contrast is therefore the mirror of the trace images. This is useful when T2 shine through is a problem. DWI quantifies cellularity based on the premise that water diffusion within the extracellular compartment is inversely related to the content and attenuation of the intracellular space (8). The higher the tumor cellularity and grade are lead to the lower the ADC and this fact is because of decreased water diffusion (4,9). However, other factors may be complicating this relationship: ADC increases with increased edema and increased edema is seen in high-grade tumors. Differences in the restriction of water movement also can result from difference in tumor cellularity (7). Clinical perfusion measurements can be made with radiotracers, but as MRI is a non-ionizing technique with high spatial and temporal resolution that can be co-registered with anatomic information, there is much interest in perfusion MRI studies. Perfusion is the regional blood flow in tissues and is defined as

the volume of blood that flows into one gram of tissue. Perfusion is a measure of the quality of vascular supply to a tissue and, since vascular supply and metabolism are usually related, perfusion can be used to measure tissue activity (5,6). Perfusion is measured using MRI by tagging the water in arterial blood during image acquisition. Tagging can be achieved either by a bolus injection of exogenous contrast agent like gadolinium, or by saturating the protons in arterial blood with RF inversion or saturation pulses. As the difference between tagged and untagged images is so small, ultra-fast imaging methods are desirable for reducing artifact. In their simple forms, perfusion images can be acquired with fast-scanning acquisitions before, during and after a bolus injection of intravenous contrast (5,7,10). In one type of this technique uses a bolus injection of gadolinium is administered intravenously during ultra-fast T2 or T2* acquisitions to evaluate perfusion. In this case, the contrast agent causes transient decreases in T2 and T2* decay in and around the microvasculature perfused with contrast. SS-GE-EPI (Single Shot-Gradient Echo-Echo Planar Imaging) sequences are usually used as they produce the required temporal resolution to measure such transient changes. In the brain, the first-pass extraction of contrast agent is zero when the blood-brain barrier (BBB) is reasonably intact, and the intravascular compartmentalization of contrast agent creates large, microscopic susceptibility gradients, and the dephasing of spins as they diffuse among them result in signal loss in T₂ and T₂*-weighted images, as first described by Villringer (10). The microscopic susceptibility gradients caused by the contrast agent, cause signal loss in a manner that depends on the type and the timing of the applied pulse

sequence. Gradient echo EPI, especially when used with echo shifting (where the TE is longer than the TR) maximizes the susceptibility effects. After data acquisition, a signal decay curve is used to ascertain blood volume, transient time and measurement of perfusion (8,11). The measured MR signal intensity change versus time curve is converted into a contrast agent tissue concentration (ΔR_2 or ΔR_2^*) versus time curve. This relationship is the key link allowing the calculation of cerebral hemodynamics. Tumor blood volume is calculated from the area under the T₂ or T₂* rate change (ΔR_2 or ΔR_2^*) and ΔR_2 (ΔR_2^*) can be calculated from signal intensity before and during the passage of contrast agent, as follows:

$$\Delta R_2 (\Delta R_2^*) = -\ln \left[\frac{S(t)}{S(0)} \right] / TE \quad \text{Eq: 1}$$

Where S (t) is MR signal at time (t), S (0) is the mean MR signal before the arrival of contrast agent, and TE is echo time. Tumor blood volume can be normalized by volume of the reference tissue (e.g. white matter) to generate an index of tumor vascularity (11). It is generally assumed that T₂ and T₂* depend upon contrast agent concentration according to the following relationship:

$$\begin{aligned} \frac{1}{T_2^*(C)} &= \frac{1}{T_2^*(0)} + CBV R^* C \\ \frac{1}{T_2(C)} &= \frac{1}{T_2(0)} + CBV R C \end{aligned} \quad \text{Eq: 2}$$

Where C is the concentration of the contrast agent in the blood, CBV is defined as the voxel volume occupied by blood vessels, and R or R* is the relaxivity of gadolinium-based contrast agent. Relaxivity depends on the molecular structure and kinetic of the complex, second sphere water exchange, and the rotational dynamics of the molecule. The T₂ and T₂* effects of a contrast agent are

almost entirely determined by its magnetic susceptibility, *i.e.* its tendency to enhance magnetic fields, so the molecular chemistry of the agent is important only to the extent that it affects susceptibility. Unfortunately, the relaxation of the agent is not certain (11,12). A theory for the 12 effects of contrast in vessels could help us to estimate R^* . According to it that R^* is not strongly dependent on tissue type as long as the blood volume is predominantly large enough in vessels, usually larger than capillaries, that diffusion is not important, and they are randomly oriented. However, been a report demonstrating that R is significantly smaller in tissues with complex microvascular structure, such as kidney and spleen than in other tissues (12). Time intensity curves for multiple images acquired during and after injection are combined to generate a cerebral blood volume (CBV) map. CBV is measured in unit of ml/100g/min and can be calculated by the integration of the concentration versus time curve. CBV reflects any increase in the cerebral capillary and venular beds, such as vasodilation or in angiogenesis (7). The angiogenic process is complex and can be stimulated by any one of several mechanisms. Typically, growth of tissue, which has outstripped its local blood supply, results in regional hypoxia and hypoglycemia that stimulates the release of local chemical messengers from the cells of the tissue itself. The best known of these messengers is the cytokine, vascular endothelial growth factor (VEGF). VEGF is a common and potent angiogenic stimulator that is found in many pathological tissues. It is released in response to local hypoglycemia and/or hypoxia and has several effects, each of which will improve metabolic supply. In the short term, VEGF will act directly on local capillaries to increase endothelial permeability resulting in an immediate increase in the

supply of nutrients (13). This increase in permeability is also believed to form an important part of the metastatic mechanism, allowing passage of tumor cells into the circulation (14). DSC provides noninvasive assessment of tumor vascularity and angiogenesis (4,8,15) through the examination of the degradation of signal intensity with time associated with the first pass of a bolus of paramagnetic contrast agent (16). Because higher vascularity corresponds to a higher tumor grade, as the grade of the astrocytoma increases, the maximum tumor CBV tends to increase (8,15). Recent developments in MRI have allowed for the assessment of cerebral blood volume (CBV) derived from perfusion-weighted MRI and perfusion abnormalities in brain tumors. An important factor in the malignancy of tumors is their ability to recruit and synthesize vascular networks for further growth and proliferation. Relative cerebral blood volume (rCBV) maps and measurements have been shown to correlate reliably with tumor grade and histological findings of increased tumor vascularity (17,18):

$$rCBV = \frac{\text{Volume of blood in a voxel}}{\text{Mass of the voxel}} \quad \text{Eq: 3}$$

The aim of this study was to evaluate the diagnostic accuracy of combined ADC and CBV values in the preoperative differentiation of diffuse Gliomas. Our objectives were as follow. 1) To calculate CBV and ADC values for diffuse Gliomas included in the study. 2) To establish whether there is any difference in rCBV and ADC values in Gliomas classified by tumor grade and histology. 3) To estimate a cut-off CBV and ADC value for differentiation of high- and low-grade Gliomas. 4) To investigate whether combined CBV and ADC values improve the diagnostic accuracy of MRI.

Materials and Methods

Patient Population

We retrospectively reviewed data obtained during a 1-year period (September 2013 - September 2014) from 19 patients with a histopathologically proved diagnosis of Glioma. They underwent an MR imaging study at our hospital (Imam Khomeini Hospital, Tehran, Iran) after signing a written informed consent.

Diagnosis was histologically confirmed by surgical resection or biopsy. The tumor specimens obtained were examined by neuropathologist and graded as low-grade (grades I and II) and high grade (grades III and IV) tumors according to the WHO Classification of Tumors of the Central Nervous System (2007) (19).

Conventional MRI

Imaging was performed with a three-tesla scanner (MAGNETOM TRIO A Tim SIEMENSE). We performed the following anatomic sequences: a 3-plane localizer sequence, T₂-tirm_tra_dark-fluid_5mm (TR_8910 ms, TE_93 ms, TI_2489 ms), T₂-tse_tra_384_5mm (TR_3230 ms, TE_93 ms), T₂-tse_sag_320_4mm (TR_4410, TE_77), T₂-tse_cro_320_4mm (TR_5510 ms, TE_77), and t1_fl2d_tra (TR_401 ms, TE_2.48 ms). All data were obtained by using 5mm thick sections with distance factor 20%, FOV read_220mm and FOV phase_75%.

PWI Parameters

Dynamic contrast-enhanced T₂^{*}-weighted gradient-echo echo-planar images were acquired during the first pass of a bolus of Dotarem, 1 mmol/mL at a dose of 0.1 mmol/kg. Nineteen sections were selected for perfusion MR imaging to cover the tumor based on T₂-weighted and FLAIR images. For the sixth acquisition, Dotarem was injected at

a rate of 4 mL/s with a power injector followed by administration of a 20-mL bolus of saline at 4 mL/s.

DWI parameters

DWI was performed before administration of contrast medium by using a multi-shot spin-echo echo-planar imaging sequence with the following parameters: TR/TE_3500/93 ms, image acquisition in the axial plane, slice thickness 4-mm, distance factor 30%, number of slice_21, FOV read 220mm, FOV phase 100mm, b-values of 0 and 1000 s/mm².

Perfusion MRI Data Evaluation

DSC images were processed by using commercially available Perfusion Map Analysis (PMA) software. The beginning and the end of the first-pass bolus were determined through inspection of the time-signal-intensity curve and care was taken to exclude any recirculation-related signal intensity. Cerebral blood volume refers to the amount of blood in a given region of brain tissue at any time, commonly measured in milliliters per 100 g of brain tissue. Because the CBV must be expressed relative to an internal reference, we normalized it by expressing ratios relative to values measured in the normal white matter of the contralateral lobe. We have referred to these relative values as rCBV. If we want to gain rCBV map, Arterial Input Function (AIF) should not be determined for bolus of contrast. Color-coded rCBV maps were generated to target regions of maximum abnormality. We placed 3 ROIs (Region of Interest) within the tumor, on areas showing the highest intratumoral rCBV on the maps. The standardized ROI was 2–3mm², which was used for most of the tumor and white matter measurements (Figure 1). Care was taken not to include large intra- or peri-tumoral vessels because these can confound perfusion measurements. The maximum rCBV value in intratumoral ROIs

was selected for quantitative analysis and correlated with corresponding specimen histopathology. This method has been demonstrated to provide the most optimal inter observer and intra observer reproducibility (20).

Diffusion MRI Data Evaluation

ADC maps and values were calculated by using commercially available PMA software with the ROIs. This software has been designed for analysis both DWI and PWI images and we can calculate ADC with draw

ROIs in ADC map on interested area of tumor. Five circular ROIs (areas ranging from 1 to 2 mm²) were manually constructed and placed over the whole tumor to select the region of the maximum hypo intensity corresponding to the solid portion of tumor. Afterward, the minimum ADC obtained was selected for the analysis. The ROIs were carefully placed to avoid cystic, necrotic, and hemorrhagic regions that might influence ADC values (Figure 1).

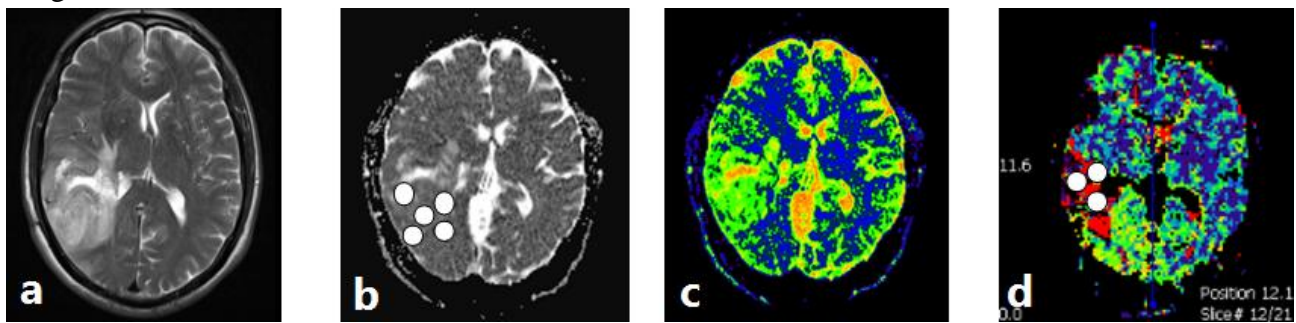


Figure 1: Images of T2 (a), ADC (b), PWI (c) and rCBV map (d) in a 47 year-old man with a right temporal grade II astrocytoma. We placed 3 ROIs within the tumor, on areas showing the highest intra-tumoral rCBV on the map, and we calculated ADC with draw five ROIs in ADC map, on interested area of tumor.

Statistical Analysis

An access database was created to track maximum rCBV, minimum ADC, and tumor grade of diffuse Gliomas. Using the Statistical Package for the Social Sciences Version 16 software (SPSS), we performed statistical analysis. At first, we check the normality of our data with Kolmogorov–Smirnov Z test. With these test we found that both group values (ADC & rCBV) have normality distribution; so mean rCBV and ADC values were compared among the tumor groups with the Standard *t* test. A $p < 0.001$ indicated a statistically significant difference. A ROC curve analysis was obtained to determine the cutoff point of rCBV and ADC values that had the best combination of specificity and sensitivity for differentiating high and low-grade Gliomas. In the ROC curve, the size of

the area under the curve indicated the degree of the relationship between rCBV or ADC values and the grade of the Gliomas: the closer to one, have stronger relationship.

Results

Patient Population

The group consisted of 19 patients (8 men and 11 women), with ages ranging from 11 to 62 years. We investigated 9 low-grade (47.37%) and 10 high-grade Gliomas (52.63%).

Evaluation of rCBV_{max} & ADC_{min} Values for Glioma Grading

rCBV values were significantly effective in grading glial tumors as low-grade and high-grade ($p = 0.0009$). Although some

overlap of distribution was shown between the values of the two groups, rCBV values were statistically different between grade II and grade IV Gliomas. ADC measurements were significantly effective in grading glial

tumors as low-grade and high-grade ($p=0.0004$). As we found in Diffusion data analysis, some overlap of distribution was shown between the ADC values of two groups. (Table1)

Table 1: The means of rCBV* and ADC** in high-grade and low-grade Gliomas

	Group	N	Range of data	Mean±SD***	Std. Mean	Error	p-value
rCBV	High	10	4.30-13.40	8.14±2.58	.81		0.0009
	Low	9	0.9-4.32	2.71±1.41	.47		
ADC	High	10	0.17-1.46	.47±.38	.12		0.0004
	Low	9	0.63-2.10	1.47±.46	.15		

* relative Cerebral Blood Volume

** Apparent Diffusion Coefficient ($\times 10^3$ mm²/s)

*** Standard Deviation

According to the ROC curves, the rCBV cutoff value of 3.85 showed high sensitivity (100%) in the characterization of high-grade Gliomas. The ADCmin cutoff value of 0.94×10^3 mm²/s generated the best combination of sensitivity (88.9%) and

specificity (90%) in the discrimination of high- and low-grade Gliomas. In that setting, the area under the ROC curve was 0.978 and 0.933 for the maximum rCBV and minimum ADC, respectively. (Figure 2).

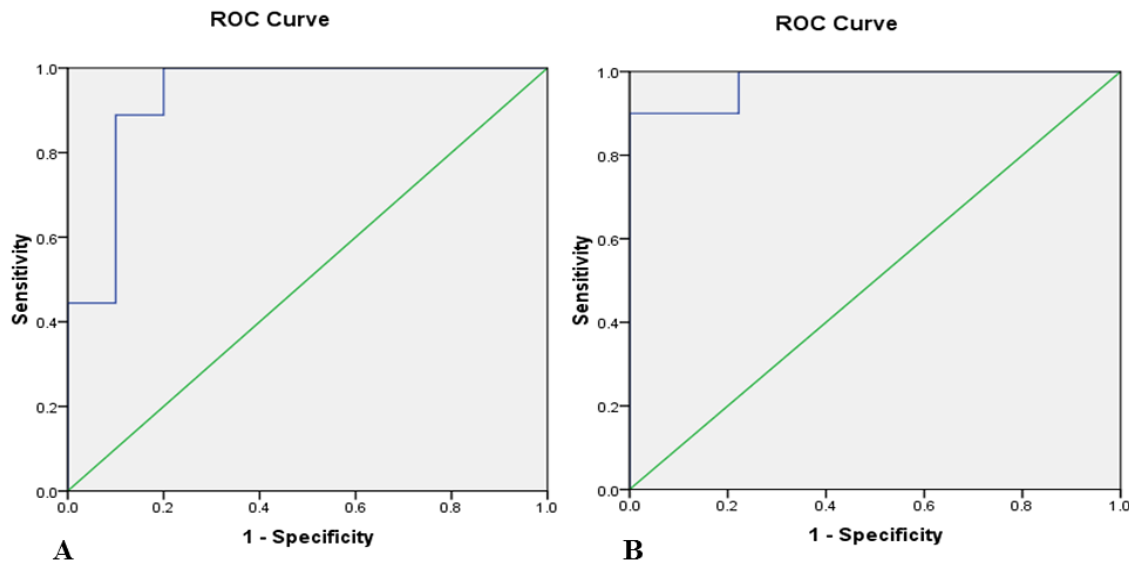


Figure 2: ROC curve analysis showing the effect of using ADC min (A) and rCBV max (B) as individual in differentiating high- and low-grade Gliomas. The area under the ROC curve for minimum ADC= 0.933, and the maximum rCBV= 0.978 respectively.

An inverse correlation has been found between ADC and rCBV with changing the grade of tumor (Figure 3).

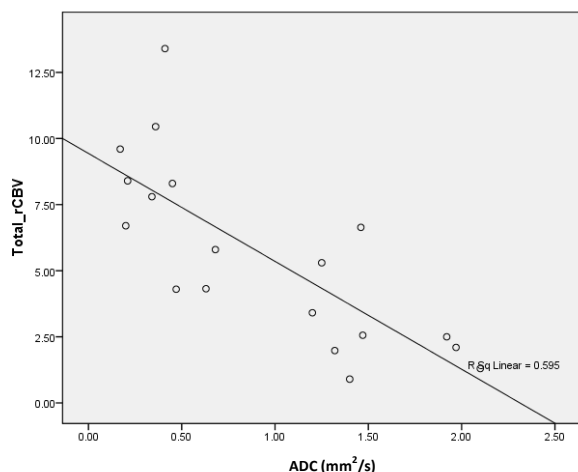


Figure 3: Inverse correlation between ADC and rCBV with changing the grade of glioma. RSq Linear=0.595

Discussion

Accurate grading of Gliomas is of importance because the therapeutic approach and prognosis differ considerably according to tumor grade (21,22). Whereas conventional MR imaging provides information on contrast enhancement, mass effect, edema, and necrosis, it is not always accurate for the precise grading of Gliomas (21). Advanced MR imaging techniques such as perfusion and diffusion MR imaging have demonstrated utility for the assessment of brain tumors (21). Thus, MR imaging perfusion methods allow the creation of CBV maps that are potentially useful in the characterization of Gliomas, because tumor aggressiveness and growth are associated with endothelial neo-vascularization. Although previous studies have suggested that contrast enhancement alone is not sufficient to predict tumor grade (23), because some low-grade Gliomas demonstrate contrast enhancement while some high-grade tumors do not (22,24). The

extent of contrast enhancement has been traditionally used as a marker of malignancy (4,22). The rCBV measurements correlate with the tumor grade and the histologic findings of increased vascularity of the tumor (21,25,26). Previous studies published between 1999 and 2005 found a range of rCBV values from 1.11 to 1.69 in low-grade Gliomas and from 3.64 to 7.32 in high-grade Gliomas, respectively. These values are comparable with our findings in our series of 19 patients, with mean rCBV values of 8.13 and 2.70 for high-grade and low-grade Gliomas, respectively. Several studies have found statistically significant discrimination between high-grade and low-grade Gliomas (21,27-29). Our findings are in agreement with these results, demonstrating significant differences in the rCBV values between high and low grade tumors. We have also found that rCBV values were statistically different between grade II and IV Gliomas. Even more, our results support histologic findings that most grade II Gliomas differ from grade IV tumors by the presence of microvascular proliferation. Similar series by Lev *et al.* (30) and Hakyemez *et al.* (3) found a sensitivity of 100% in discriminating the high- and low-grade tumors with the use of 1.5 and 2 as the rCBV threshold value, respectively. A series published in 2005 by Calli C, *et al.* found the rCBV threshold value of 1.75 with a sensitivity of 95% and specificity of 57.5% (31). In our study of 19 Gliomas, we found similar results to those of Law *et al.* (sensitivity, 94.4%; specificity, 50%) using a cutoff value of 1.74 (14). Our results are also in agreement with those published by Lev *et al.* (32) and show us that as the threshold level is lowered, the specificity is decreased and some low-grade Gliomas are falsely identified as high-grade and will be treated

more aggressively. In our group of patients, on the other hand, sensitivity decreased to 91.2% when the rCBV cutoff value was increased to 3.29. These results are in agreement with those published by Shin *et al.* who reported 91% sensitivity and 83% specificity for a cutoff value of 2.9 in a group of 19 Gliomas (33). With these cutoff values, some high-grade Gliomas would be misidentified as low-grade tumors and would be treated conservatively, resulting in a potentially rapid death. Some authors suggested that quantitative perfusion imaging predicts tumor biologic activity and survival better than histopathologic grade does. We are in agreement with the above argument that DSC can be used to predict clinical outcome in patients with low-grade Gliomas, independent of pathologic findings. DWI allows assessing the cellularity of tumors in a noninvasive form; because cellular and subcellular elements impede water mobility (34) and quantitative information from the restriction of water molecule movement can be observed in calculating the ADC (35,36). Thus, brain neoplasms with higher cellularity or with a higher grade show a significant reduction in ADC values (36,37). In our series of 19 Gliomas, we found a significant difference in the minimum ADC value for differentiating the low and high-grade Gliomas. These findings are similar to those reported previously by Lee *et al.* (n=16) (22), Kono *et al.* (n=17) (35), and Calli *et al.* (n=31) (31), with high-grade Gliomas showing a significant reduction in ADC values and increased signal intensity on DWI. Our findings also agree with those demonstrated by Yamasaki *et al.*; this similarity suggests an inverse relationship between ADC and glial tumors of WHO grades II–IV (38). Most of the published

studies to date have evaluated the diffusion properties in high- and low-grade Gliomas. We have gone one-step further and have studied the ADC values in the Gliomas classified by grade and histology. According to this, ADC measurements are better than rCBV values in distinguishing the grades of Gliomas and astrocytic tumors. In our experience, the mean ADC value was $0.475 \times 10^3 \text{ mm}^2/\text{s}$ for high grade Gliomas and lower than ADC values published by Stadnik *et al.* who reported the mean ADC values of $1.14 \times 10^3 \text{ mm}^2/\text{s}$ (39). The reason for our lower ADC values may be that we always sampled the minimum ADC value from the solid portion of the tumor. The cutoff value of $0.94 \times 10^3 \text{ mm}^2/\text{s}$ for the minimum ADC generated the best combination of sensitivity (88.9%) and specificity (90%) in the discrimination of high- and low grade Gliomas. In the present study, we were interested in determining whether combined data from rCBV and ADC values could improve the diagnostic accuracy of perfusion and diffusion alone. An inverse correlation has been found between ADC and rCBV with changing the grade of tumor. This comes back to histopathological characteristics of cell tumors. With increase the grade of tumor, we can see a large increase in number of cells. Therefore, it causes a decrease in the extra space between cells, so restriction in water molecules motion and decrease in ADC values. In the other hand, we can see an increase in the vascularization of tumor tissue and total volume of blood in them. Therefore we can see this inverse correlation.

This was the work that the combination of diffusion and perfusion MR imaging has been used as a diagnostic tool in the presurgical evaluation of Gliomas. Our results show that the area under the ROC curve for the

maximum rCBV was 0.978 and 0.933 for the minimum ADC. According to these results, the classification accuracy based on maximum rCBV was higher than that based on minimum ADC, we may conclude that the combination of ADC and rCBV values increases the diagnostic accuracy of MR imaging in the preoperative grading of Gliomas. Kim et al. also found an adjunctive value of perfusion MR imaging (pulsed arterial spin-labeling) and ADC scoring in the Glioma grading compared with conventional images alone (26). However, there have been few reports of the simultaneous use of perfusion and diffusion imaging in Glioma grading, and further studies will be needed. There are some limitations in our study. First, stereotactic biopsies were not targeted by rCBV or ADC maps. Second, there is the possibility of histopathologic misdiagnosis attributable to sampling error in the pathologic examination because of the histologic heterogeneity of tumor tissues. It is widely known that a given individual Glioma, usually of high grade, often contains a continuum of histologic features of grades II-IV and tumor grading is dependent on the site of tumor biopsy or resection and thus subject to sampling error or under sampling.

Conclusion

Our results showed that ADC and rCBV maps could be used as a noninvasive method of evaluation of tumor grade. We have found that rCBV measurements are better than ADC values in distinguishing the grades of Glioma. Although further studies will be needed to confirm the utility of combined diffusion weighted and perfusion MR imaging, the results also suggested that the combination of minimum ADC and maximum rCBV

improves the diagnostic accuracy of MR imaging in the preoperative determination of Glioma grade.

Acknowledgements

The authors are grateful to Mehdi Ghiasi for expert technical assistance. In addition, authors would like to thank the patients for participating in this study and signing written informed consent for its publication.

Conflict of Interest

The authors have no conflict of interest.

References

1. Fuller GN, Scheithauer BW. The 2007 Revised World Health Organization (WHO) Classification of Tumours of the Central Nervous System: Newly Codified Entities. *Brain Pathol* 2007; 17(3): 304-7.
2. Kleihues P, Louis DN, Scheithauer BW, Rorke LB, Reifenberger G, Burger PC, et al. The WHO Classification of Tumors of the Nervous System. *J Neuropathol Exp Neurol* 2002; 61(3):215-25.
3. Hakyemez B, Erdogan C, Ercan I, Ergin N, Uysal S, Atahan S. High-Grade and Low-Grade Gliomas: Differentiation by Using Perfusion MR Imaging. *Clin Radiol* 2005; 60(4): 493-502.
4. Sadeghi N, D'Haene N, Decaestecker C, Levivier M, Metens T, Maris C. Apparent Diffusion Coefficient and Cerebral Blood Volume in Brain Gliomas: Relation to Tumor Cell Density and Tumor Microvessel Density Based on Stereotactic Biopsies. *AJNR Am J Neuroradiol* 2008; 29(3): 476-82.
5. Le Bihan D, Johansen-Berg H. Diffusion MRI at 25: Exploring Brain Tissue Structure and Function. *Neuroimage* 2012; 61(2): 324-41.
6. Mori S, Zhang J. Principles of Diffusion Tensor Imaging and its Applications to Basic Neuroscience Research. *Neuron* 2006; 51(5): 527-39.

7. Yuh WT, Christoforidis GA, Koch RM, Sammet S, Schmalbrock P, Yang M, et al. Clinical Magnetic Resonance Imaging of Brain Tumors at Ultrahigh Field: a State-of-the-Art Review. *Top Magn Reson Imaging* 2006; 17(2): 53-61.
8. Cha S. Update on Brain Tumor Imaging: from Anatomy to Physiology. *AJNR Am J Neuroradiol* 2006; 27(3): 475-87.
9. Gupta RK, Cloughesy TF, Sinha U, Garakian J, Lazareff J, Rubino G, et al. Relationships between Choline Magnetic Resonance Spectroscopy, Apparent Diffusion Coefficient and Quantitative Histopathology in Human Glioma. *J Neurooncol* 2000; 50(3): 215-26.
10. Villringer A, Rosen BR, Belliveau JW, Ackerman JL, Lauffer RB, Buxton RB, et al. Dynamic Imaging with Lanthanide Chelates in Normal Brain: Contrast Due to Magnetic Susceptibility Effects. *Magn Reson Med* 1988; 6(2): 164-74.
11. Uematsu H, Maeda M. Double-Echo Perfusion-Weighted MR Imaging: Basic Concepts and Application in Brain Tumors for the Assessment of Tumor Blood Volume and Vascular Permeability. *Eur Radiol* 2006; 16(1): 180-6.
12. Johnson KM, Tao JZ, Kennan RP, Gore JC. Intravascular Susceptibility Agent Effects on Tissue Transverse Relaxation Rates *In Vivo*. *Magn Reson Med* 2000; 44(6): 909-14.
13. Shweiki D, Neeman M, Itin A, Keshet E. Induction of Vascular Endothelial Growth Factor Expression by Hypoxia and by Glucose Deficiency in Multicell Spheroids: Implications for Tumor Angiogenesis. *Proc Natl Acad Sci USA* 1995; 92(3): 768-72.
14. Law M, Yang S, Wang H, Babb JS, Johnson G, Cha S, et al. Glioma Grading: Sensitivity, Specificity, and Predictive Values of Perfusion MR Imaging and Proton MR Spectroscopic Imaging Compared with Conventional MR Imaging. *AJNR Am J Neuroradiol* 2003; 24(10): 1989-98.
15. Hirai T, Murakami R, Nakamura H, Kitajima M, Fukuoka H, Sasao A, et al. Prognostic Value of Perfusion MR Imaging of High-Grade Astrocytomas: Long-Term Follow-Up Study. *AJNR Am J Neuroradiol* 2008; 29(8): 1505-10.
16. Cha S, Knopp EA, Johnson G, Wetzel SG, Litt AW, Zagzag D. Intracranial Mass Lesions: Dynamic Contrast-Enhanced Susceptibility-Weighted Echo-Planar Perfusion MR Imaging. *Radiology* 2002; 223(1): 11-29.
17. Andersen C, Jensen FT. Differences in Blood-Tumour-Barrier Leakage of Human Intracranial Tumours: Quantitative Monitoring of Vasogenic Oedema and its Response to Glucocorticoid Treatment. *Acta Neurochir (Wien)* 1998; 140(9): 919-24.
18. Lund EL, Spang-Thomsen M, Skovgaard-Poulsen H, Kristjansen PE. Tumor Angiogenesis-a New Therapeutic Target in Gliomas. *Acta Neurol Scand* 1998; 97(1): 52-62.
19. Louis DN, Ohgaki H, Wiestler OD, Cavenee WK, Burger PC, Jouvet A, et al. The 2007 WHO Classification of Tumours of the Central Nervous System. *Acta Neuropathol* 2007; 114(2):97-109.
20. Wetzel SG, Cha S, Johnson G, Lee P, Law M, Kasow DL, et al. Relative Cerebral Blood Volume Measurements in Intracranial Mass Lesions: Interobserver and Intraobserver Reproducibility Study. *Radiology* 2002; 224(3): 797-803.
21. Rollin N, Guyotat J, Streichenberger N, Honnorat J, Tran Minh VA, Cotton F. Clinical Relevance of Diffusion and Perfusion Magnetic Resonance Imaging in Assessing Intra-Axial Brain Tumors. *Neuroradiology* 2006; 48(3): 150-9.
22. Lee EJ, Lee SK, Agid R, Bae JM, Keller A, Terbrugge K. Preoperative Grading of Presumptive Low-Grade Astrocytomas on MR Imaging: Diagnostic Value of Minimum Apparent Diffusion Coefficient. *AJNR Am J Neuroradiol* 2008; 29(10): 1872-7.
23. Knopp EA, Cha S, Johnson G, Mazumdar A, Golfinos JG, Zagzag D, et al. Glial Neoplasms: Dynamic Contrast-Enhanced T2*-weighted MR Imaging. *Radiology* 1999; 211(3): 791-8.
24. McKnight TR, Lamborn KR, Love TD, Berger MS, Chang S, Dillon WP, et al. Correlation of Magnetic Resonance Spectroscopic and Growth Characteristics within Grades II and III Gliomas. *J Neurosurg* 2007; 106(4): 660-6.

25. Kao HW, Chiang SW, Chung HW, Tsai FY, Chen CY. Advanced MR Imaging of Gliomas: An Update. *Biomed Res Int* 2013; 2013: 970586.
26. Kim HS, Kim SY. A Prospective Study on the Added Value of Pulsed Arterial Spin-Labeling and Apparent Diffusion Coefficients in the Grading of Gliomas. *AJNR Am J Neuroradiol* 2007; 28(9): 1693-9.
27. Law M, Yang S, Babb JS, Knopp EA, Golfinos JG, Zagzag D, et al. Comparison of Cerebral Blood Volume and Vascular Permeability from Dynamic Susceptibility Contrast-Enhanced Perfusion MR Imaging with Glioma Grade. *AJNR Am J Neuroradiol* 2004; 25(5): 746-55.
28. Boxerman JL, Schmainda KM, Weisskoff RM. Relative Cerebral Blood Volume Maps Corrected for Contrast Agent Extravasation Significantly Correlate with Glioma Tumor Grade, Whereas Uncorrected Maps Do Not. *AJNR Am J Neuroradiol* 2006; 27(4): 859-67.
29. Bulakbasi N, Kocaoglu M, Farzaliyev A, Tayfun C, Ucoz T, Somuncu I. Assessment of Diagnostic Accuracy of Perfusion MR Imaging in Primary and Metastatic Solitary Malignant Brain Tumors. *AJNR Am J Neuroradiol* 2005; 26(9): 2187-99.
30. Lev MH, Rosen BR. Clinical Applications of Intracranial Perfusion MR Imaging. *Neuroimaging Clin N Am* 1999; 9(2): 309-31.
31. Calli C, Kitis O, Yuntan N, Yurtseven T, Islekel S, Akalin T. Perfusion and Diffusion MR Imaging in Enhancing Malignant Cerebral Tumors. *Eur J Radiol* 2006; 58(3): 394-403.
32. Lev MH, Ozsunar Y, Henson JW, Rasheed AA, Barest GD, Harsh GR, et al. Glial Tumor Grading and Outcome Prediction Using Dynamic Spin-Echo MR Susceptibility Mapping Compared with Conventional Contrast-Enhanced MR: Confounding Effect of Elevated rCBV of OligodendroGliomas. *AJNR Am J Neuroradiol* 2004; 25(2): 214-21.
33. Shin JH, Lee HK, Kwun BD, Kim JS, Kang W, Choi CG, et al. Using Relative Cerebral Blood Flow and Volume to Evaluate the Histopathologic Grade of Cerebral Gliomas: Preliminary Results. *AJR Am J Roentgenol* 2002; 179(3): 783-9.
34. Kwee TC, Galbán CJ, Tsien C, Junck L, Sundgren PC, Ivancevic MK, et al. Comparison of Apparent Diffusion Coefficients and Distributed Diffusion Coefficients in High-Grade Gliomas. *J Magn Reson Imaging* 2010; 31(3): 531-7.
35. Kono K, Inoue Y, Nakayama K, Shakudo M, Morino M, Ohata K, et al. The Role of Diffusion-Weighted Imaging in Patients with Brain Tumors. *AJNR Am J Neuroradiol* 2001; 22(6): 1081-8.
36. Kitis O, Altay H, Calli C, Yuntan N, Akalin T, Yurtseven T. Minimum Apparent Diffusion Coefficients in the Evaluation of Brain Tumors. *Eur J Radiol* 2005; 55(3): 393-400.
37. Sugahara T, Korogi Y, Kochi M, Ikushima I, Shigematu Y, Hirai T, et al. Usefulness of Diffusion-Weighted MRI with Echo-Planar Technique in the Evaluation of Cellularity in Gliomas. *J Magn Reson Imaging* 1999; 9(1): 53-60.
38. Yamasaki F, Kurisu K, Satoh K, Arita K, Sugiyama K, Ohtaki M, et al. Apparent Diffusion Coefficient of Human Brain Tumors at MR Imaging. *Radiology* 2005; 235(3): 985-91.
39. Stadnik TW, Chaskis C, Michotte A, Shabana WM, van Rompaey K, Luybaert R, et al. Diffusion-Weighted MR Imaging of Intracerebral Masses: Comparison with Conventional MR Imaging and Histologic Findings. *AJNR Am J Neuroradiol* 2001; 22(5): 969-76.